

$$x = \begin{bmatrix} x_{c_0}^T & \cdots & x_{c_N}^T & \lambda_{f_1} & \cdots & \lambda_{f_M} \end{bmatrix}^T$$

$$x_{c_k} = \begin{bmatrix} G p_{I_k}^T & G v_{I_k}^T & G_{I_k} q^T & b_{a_k}^T & b_{g_k}^T \end{bmatrix}^T$$

The state variables of structureless VIO is obtained by deleting the environmental feature points. Structureless VIO can be expressed as

$$\min_x \left\{ \|r_p\|^2 + \sum_{k=1}^N \|r_{I_{k-1,k}}\|_{\Sigma_{I_{k-1,k}}}^2 + \sum_{l=1}^M \sum_{(i,j) \in \mathcal{K}^l} \rho_{Hub} \left(\|r_{ij}^n\|_{\Sigma_C}^2 \right) \right\}$$

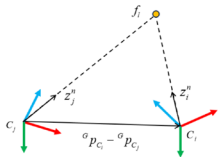


Fig. 1: Epipolar constraint.



Fig. 2: Corridor scene.

$$r_{ij}^n(x_{c_i}, x_{c_j}) = \left(G_{I_j} R_C^I R z_j^n \right)^T \left[\frac{t}{\|t\|} \right]_{\times} \left(G_{I_i} R_C^I R z_i^n \right)$$

$$t = G p_{C_i} - G p_{C_j}$$

$$= G p_{I_i} + G_{I_i} R^I p_C - G p_{I_j} - G_{I_j} R^I p_C$$

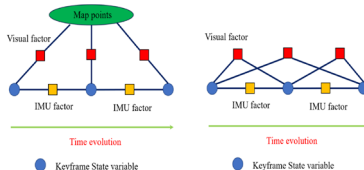


Fig. 3: Left: factor graph for classical structure-based VI-BA. Right: factor graph for novel structureless VI-BA.

Performance comparison on TUM-VI Dataset.

Sequence	ATE (m)		Avg solve time (ms)	
	VINS-Mono	Ours	VINS-Mono	Ours
room1	0.067	0.051	20.19	11.56
room2	0.068	0.104	22.67	12.58
room3	0.121	0.114	19.73	11.89
room4	0.048	0.063	21.03	13.14
room5	0.217	0.127	18.17	11.27
room6	0.076	0.085	26.24	15.04
Avg	0.100	0.091	21.34	12.58
corridor1	0.629	0.398	18.62	11.46
corridor2	0.933	0.956	19.06	12.13
corridor3	1.978	0.893	16.75	10.98
corridor4	0.315	0.224	19.92	12.69
corridor5	0.689	0.456	19.56	12.36
Avg	0.909	0.585	18.78	11.92

- A novel structureless VIO that adopts epipolar constraint instead of reprojection error or photometric error.
- Results demonstrate that our method reduces the optimization time by a large margin and offers improvement in accuracy.